



MINISTRY OF DEFENCE (PROCUREMENT EXECUTIVE)
AERONAUTICAL RESEARCH COUNCIL
CURRENT PAPERS

Experimental Investigation of a High-Lift Low-Drag Aerofoil

By

F. H. Kelling

*Dept. of Aeronautics and Fluid Mechanics,
The University of Glasgow*

LONDON HER MAJESTY'S STATIONERY OFFICE

1971

Price 60p net

EXPERIMENTAL INVESTIGATION OF A HIGH-LIFT
LOW-DRAG AEROFOIL

by

F. H. Kelling
Dept. of Aeronautics and Fluid Mechanics,
The University of Glasgow

SUMMARY

One of a series of low-drag aerofoils¹ designated GU 25-5(11)8 was selected for low speed wind tunnel testing at Reynolds numbers around half a million. Coefficients of lift, drag and pitching moment were obtained for a range of incidence, using a two-dimensional wing. The maximum section lift coefficient obtained was 1.93 and the minimum profile drag coefficient was 0.0112. Results compared favourably with those deduced theoretically. The addition of a boundary layer trip to the upper surface caused the profile drag to decrease at some incidences. At the design lift coefficient of 1.4, the ratio of lift to profile drag was 108 at a Reynolds number of 0.63 million. The addition of an extended, sealed, flat-plate flap, with a chord one tenth that of the aerofoil, at the trailing edge of the aerofoil gave favourable results. A maximum ratio of lift to profile drag of 116 was obtained at a lift coefficient of 1.8 with a flap deflection of 17.8 degrees, while the maximum lift coefficient achieved was 2.30.

* Replaces A.R.C. 30 983

LIST OF CONTENTS

Page

Notation	3
1. Introduction	5
2. Testing Procedure and Technique	7
3. Presentation of Results	8
4. Discussion	12
5. Acknowledgements	16
References	17
Appendix 1	18
Appendix 2	19
Figure 1: GU 25-5(11)8 Aerofoil	
" 2: Lift Coefficient versus Geometric Incidence	
" 3: Pressure Drag Coefficient versus Geometric Incidence	
" 4: Moment Coefficient about the Leading Edge versus Geometric Incidence	
" 5: Profile Drag Coefficient versus Geometric Incidence	
" 6: Corrected Lift Coefficient versus Corrected Incidence	
" 7: Corrected Lift Coefficient versus Corrected Profile Drag Coefficient	
" 8: Corrected Lift Coefficient versus Corrected Pitching Moment Coefficient about the Quarter Chord	
" 9: Pressure Distributions, Plain Aerofoil	
" 10: Pressure Distributions, Aerofoil with Trip	
" 11: Pressure Distributions at Design Lift Coefficient	
" 12: Pressure Distributions, Aerofoil with Flap	
" 13: Reynolds Number when Wake Characteristics change versus Corrected Incidence, Aerofoil with Trip	
" 14: Comparison of GU 25-5(11)8 Polars with others	
" 15: Photograph of Aerofoil Upper Surface with Oil Film	

NOTATION

c	aerofoil chord length
C_{D_P}'	normal pressure drag coefficient
C_D'	profile drag coefficient
C_{D_V}	vortex drag coefficient
C_D	profile drag coefficient corrected
C_L'	lift coefficient
C_L	lift coefficient corrected
$C_{M_{L.E.}}'$	pitching moment coefficient about the leading edge
$C_{M_{c/4}}'$	pitching moment coefficient about the quarter chord
$C_{M_{c/4}}$	pitching moment coefficient about the quarter chord, corrected.
C_P	pressure coefficient
N	wind tunnel fan speed in revolutions per minute
q_α	surface velocity relative to that of free stream
R	Reynolds number, U_{oc}/ν
t	maximum thickness of the aerofoil
U_0	free stream velocity
x	distance chordwise from the leading edge (positive rearwards)
y	distance normal to the aerofoil chord (positive upwards)
x_1	chordwise position of the aerodynamic centre aft of the quarter chord as a fraction of the chord
y_1	perpendicular distance of the aerodynamic centre above the chord line as a fraction of the chord
α^1	geometric incidence corrected for the yawed airstream in the tunnel working section
α_e	effective incidence of the aerofoil in two-dimensional flow

α	effective incidence corrected for streamline curvature
α_0	angle of zero lift
δ	flap deflection
Δ	increment due to flap deflection
KI	slope of wing surface relative to chord line
THETA	angular co-ordinate of the point on the unit circle into which aerofoil is mapped by conformal transformation
ν	fluid kinematic viscosity

1. Introduction

The aerofoil in question, Fig.1, was one of a series designed by T. Nonweiler¹ and was designated GU 25-5(11)8. It had a maximum thickness to chord ratio of 20%, occurring at 41.6% chord from the leading edge. The design lift coefficient was 1.39 with the theoretical low drag range extending from $C_L = 0.89$ to $C_L = 1.89$. The maximum camber to chord ratio was 7.1% and occurred at 46.4% chord from the leading edge. The trailing edge angle was 23.2 degrees. This feature, together with the fairly flat undersurface and the absence of concavities, was planned to ease practical problems in wing construction.

The wind tunnel model had a chord of 0.305 m and a span of 0.84 m so that it could be positioned vertically in the working section of the Department's low-speed wind tunnel. The working section dimensions are nominally, height 0.84 m, breadth 1.14 m. The turbulence intensity,

$\sqrt{u'^2} / U_0$, in the test section is 0.5%. The aerofoil model was constructed in the conventional manner using wood laminations and the actual ordinates were within 0.15 mm of the values stated in Table 1. The model had 32 pressure tappings on its surface at or near the mid-span; their co-ordinates are given in Table 2, and their positions are indicated on Fig.1.

The model was tested to ascertain the section lift, profile drag and pitching moment characteristics over a limited range of Reynolds numbers between 0.4×10^6 and 0.7×10^6 . The effect of a boundary layer trip on the upper surface of the aerofoil was investigated. The aerodynamic characteristics were also obtained for the aerofoil fitted with extended sealed flaps set at four different angles. In each case the flap chord was one tenth of the aerofoil chord. Fig.1 gives the position of the trip and the flap arrangement.

Table 1/

Table 1. Aerofoil Model Co-ordinates

x/c	y/c	x/c	y/c	x/c	y/c
1.000	0.000	0.200	0.134	0.300	-0.031
0.950	0.018	0.150	0.116	0.350	-0.031
0.900	0.036	0.100	0.093	0.400	-0.030
0.850	0.054	0.075	0.079	0.450	-0.028
0.800	0.073	0.050	0.062	0.500	-0.026
0.750	0.092	0.025	0.041	0.550	-0.024
0.700	0.110	0.005	0.016	0.600	-0.021
0.650	0.128	0.000	0.000	0.650	-0.019
0.600	0.144	0.005	-0.010	0.700	-0.016
0.550	0.158	0.025	-0.018	0.750	-0.014
0.500	0.168	0.050	-0.023	0.800	-0.011
0.450	0.171	0.075	-0.025	0.850	-0.009
0.400	0.170	0.100	-0.027	0.900	-0.007
0.350	0.166	0.150	-0.030	0.950	-0.004
0.300	0.158	0.200	-0.031	1.000	-0.000
0.250	0.148	0.250	-0.031		

Note A complete set of co-ordinate data for this aerofoil is given in Appendix 1.

Table 2/

Table 2. Co-ordinates of Pressure Tappings

Tap No.	x/c	y/c	Tap No.	x/c	y/c	Tap No.	x/c	y/c
1	0.966	0.012	12	0.089	0.086	23	0.096	-0.028
2	0.882	0.042	13	0.044	0.057	24	0.171	-0.031
3	0.806	0.070	14	0.014	0.028	25	0.263	-0.032
4	0.721	0.102	15	0.005	0.015	26	0.365	-0.030
5	0.633	0.134	16	0.000	0.003	27	0.473	-0.028
6	0.547	0.158	17	0.000	0.000	28	0.584	-0.022
7	0.463	0.170	18	0.001	-0.006	29	0.692	-0.017
8	0.379	0.168	19	0.005	-0.010	30	0.791	-0.012
9	0.296	0.157	20	0.012	-0.014	31	0.875	-0.008
10	0.217	0.139	21	0.021	-0.018	32	0.965	-0.003
11	0.148	0.114	22	0.040	-0.022			

2. Testing Procedure and Technique

2.1 Lift, pressure drag and pitching moment

The pressure distribution at the mid-section of the model was obtained at various incidences for working section wind speeds of 18, 24 and 30 m/s with the following configurations.

- a) Basic aerofoil
- b) Aerofoil with a boundary layer trip of 0.13 mm diameter varnished thread on the upper surface at 0.455 c from the leading edge measured along the chord
- c) Aerofoil fitted with extended sealed flat plate flaps with angles of 7.7, 17.8 and 27.8 degrees respectively.

One test was also run at the middle speed with a -11.5 degree flap fitted. Although all these tests were run with the trip in position, the 7.7 degree flap was also tested on the basic aerofoil without the trip.

The/

The pressure distributions were obtained with the aid of a multitube liquid manometer. The average wall pressure in the working section ahead of the model was used as the reference (reservoir) pressure. The maximum pressure difference obtained was taken as the stream dynamic pressure and this figure was used to calculate pressure coefficients. The dynamic pressures so obtained compared favourably with the test section dynamic pressures deduced conventionally. The integrations of the pressure distribution were done by using the University's KDF 9 computer. The pressure distribution data thus yielded lift coefficient, pressure drag coefficient and the pitching moment coefficient about the leading edge for each incidence.

2.2 Profile drag coefficient

A pitot comb was used to estimate the profile (or boundary layer) drag coefficient of the section. The tips of the pitot tubes were located at one chord length aft of the model trailing edge. A tilting multitube manometer was used to record the various pressures and the boundary layer drag coefficient was evaluated by using the method outlined in Ref.2.

2.3 Flow visualisation

At one stage in the investigation, an oil film technique³ was used to ascertain the location and breadth of the separation bubble on the upper surface of the aerofoil and to examine the effect of fitting a variety of boundary layer trips. The technique was also used to study the behaviour of the boundary layer on the aerofoil upper surface near the wind tunnel walls. Photographs were taken of some of the ensuing flow patterns, Fig.15.

3. Presentation of Results

3.1 Graphs

The results are shown graphically in Figs.2 to 15. Figs.2 to 5 present the results obtained directly from the test data before any corrections were applied. The corrected values are then shown in Figs.6 to 8. It should be noted that Fig.8 depicts the corrected pitching moment coefficient about the quarter chord in contrast to Fig.4 which shows the uncorrected moment coefficient about the leading edge. Each graph from Figs.2 to 8 contains a set of curves for each of the three test Reynolds numbers. The various curves were drawn using results obtained from the aerofoil configurations indicated in 2.1.

Figs.9 to 12 show plots of the chordwise distribution of the pressure coefficient for various aerofoil incidences and configurations. All, except Fig.12, pertain to the highest test Reynolds number. Fig.11 affords a comparison of theory with experiment at the design lift coefficient. The ideal flow pressure distribution was obtained using Ref.1. That for viscous flow was produced by the University's computer using the "Powell" program⁹ kindly sent to us from the National Physical Laboratory by D. J. Hall. The pressure distributions shown in Fig.12 for the flapped aerofoil are at what appears to be the optimum Reynolds number for this configuration. The pressure plots given in Fig.12 are all at the fairly high incidence of 12.6 degrees. It is to be noted that, with the flaps, the overall chord increases, so that the values of x/c for the pressure tapping differ slightly from those for the aerofoil alone.

Fig.13 gives the limits of Reynolds number and incidence at which low profile drag is obtained for the aerofoil fitted with trip. The boundaries were found by varying the speed at each incidence and observing when the wake breadth and total head changed abruptly. The value of the critical speed depended on whether the wind speed was being increased or decreased.

Fig.14 compares the lift and profile drag characteristics of the aerofoil under test with those obtained from a low-drag aerofoil designated FX 05-H-126 by Wortmann⁶ and NACA 63₄-420 fitted with a 0.25 c slotted flap at 20 degrees⁷. It should be noted that the Reynolds numbers for the curves are not similar. A theoretical curve for the G.U. aerofoil at $R = 0.63 \times 10^6$, using the "Powell" program mentioned earlier, is also included.

3.2 Lift and profile drag

The following Table gives the values of the average lift curve slope, $\frac{dC_L}{d\alpha}$ (where α is in degrees), for the various tests:

Table 3

Average value of Reynolds Number	0.41×10^6	0.53×10^6	0.66×10^6
Basic aerofoil with and without trip	0.100	0.107	0.114
Trip, 0.1 c extended flap, $\delta = -11.5$ degrees	-	0.098	-
Trip, 0.1 c extended flap, $\delta = 7.7$ degrees	0.100	0.108	0.112
Trip, 0.1 c extended flap, $\delta = 17.8$ degrees	0.098	0.102	0.108
Trip, 0.1 c extended flap, $\delta = 27.8$ degrees	0.097	0.094	0.092

The angle of zero lift can only be stated for the basic aerofoil at the highest Reynolds number and that by extrapolation. Without the trip, α_0 was about 6.4 degrees while the value for the aerofoil with the trip was about 6.0 degrees.

The following Table gives the maximum lift coefficient and the incidence at which it occurred for each test.

Table 4/

Table 4

Average value of Reynolds Number		0.41×10^6	0.53×10^6	0.66×10^6
Basic aerofoil	Max C_L	1.93	1.90	1.85
	α	12.3°	12.2°	11.2°
With trip	Max C_L	1.93	1.85	1.88
	α	12.3°	11.2°	11.8°
Trip, flap at 7.7°	Max C_L	2.02	2.03	2.04
	α	12.0°	11.0°	11.0°
Trip, flap at 17.8°	Max C_L	2.26	2.18	2.11
	α	11.2°	10.4°	10.2°
Trip, flap at 27.8°	Max C_L	2.30	2.27	2.18
	α	10.6°	10.0°	10.1°

As a comparison the next table gives a tentative value for the lift coefficient at the drag rise incidence which is also noted together with the corresponding profile drag coefficient.

Table 5

Average value of Reynolds Number		0.41×10^6	0.53×10^6	0.66×10^6
Basic aerofoil	C_L	1.92	1.86	1.84
	α	12.2°	11.0°	10.8°
	C_D	.0225	.0185	.0153
With trip	C_L	1.93	1.85	1.88
	α	12.3°	11.2°	11.8°
	C_D	.0235	.0190	.0175
Trip, flap at 7.7°	C_L	1.95	2.02	2.01
	α	10.6°	10.4°	10.3°
	C_D	.0223	.0192	.0210
Trip, flap at 17.8°	C_L	2.18	2.16	2.06
	α	9.8°	9.8°	9.2°
	C_D	.0221	.0210	.0190
Trip, flap at 27.8°	C_L	2.26	2.26	2.13
	α	9.4°	9.6°	9.3°
	C_D	.0265	.0215	.0215

The minimum profile drag coefficient is noted in the next Table together with the incidence at which it occurred and the corresponding lift coefficient. This information can only be given for the aerofoil without flaps since the flapped aerofoil was not tested at the lower values of lift coefficient.

Table 6

Reynolds Number		0.39×10^6	0.50×10^6	0.63×10^6
Basic aerofoil	Min. C_D	.0148	.0136	.0112
	α	1.4°	1.2°	1.4°
	C_L	0.88	0.87	0.86
With trip	Min. C_D	.0127	.0113	.0112
	α	1.5°	1.4°	2.0°
	C_L	0.90	0.89	0.86

3.3 Pitching moment

The slopes of the quarter chord pitching moment and lift coefficient curves ($d C_{M_{c/4}} / d C_L$) are noted in the next Table for the various tests.

The values given are tentative and refer to the "working" range of incidence.

Table 7

Average Reynolds Number	0.41×10^6	0.53×10^6	0.66×10^6
Basic aerofoil	+ .005	0	- .030
With trip	+ .005	0	- .020
Trip, flap at 7.7°	- .005	- .015	- .020
Trip, flap at 17.8°	+ .010	+ .012	+ .014
Trip, flap at 27.8°	+ .030	+ .050	+ .060

For the basic aerofoil the position of the aerodynamic centre (x_1, y_1) was calculated using the expression

$$\left[\left(1 + C_D \frac{d\alpha}{dC_L} \right) \cos \alpha + \left(\frac{dC_D}{dC_L} - C_L \frac{d\alpha}{dC_L} \right) \sin \alpha \right] x_1 - \left[\left(\frac{dC_D}{dC_L} - C_L \frac{d\alpha}{dC_L} \right) \cos \alpha - \left(C_D \frac{d\alpha}{dC_L} + 1 \right) \sin \alpha \right] y_1 = - \frac{dC_{M_{c/4}}}{dC_L} \dots (10)$$

and/

and inserting the appropriate values: x_1 is the chordwise position of the aerodynamic centre aft of the quarter chord as a fraction of the chord and y_1 is the perpendicular distance of the aerodynamic centre above the chord line, again as a fraction of the chord. The results were as follows:

	x_1	y_1
$R = 0.39 \times 10^6$	- .004	- .003
$R = 0.50 \times 10^6$	0	0
$R = 0.63 \times 10^6$.029	.007

The co-ordinates of the aerodynamic centre for the aerofoil with trip are:

	x_1	y_1
$R = 0.39 \times 10^6$	- .005	- .001
$R = 0.50 \times 10^6$	0	0
$R = 0.63 \times 10^6$.020	.003

4. Discussion

4.1 Comparison with theory

4.1.1 Basic aerofoil

The theoretical results for this aerofoil in inviscid flow were computed and are stated below.

Zero lift incidence α_0	-6.11 degrees
Lift curve slope per degree, $dC_L/d\alpha$	0.127
Lower limit of C_L	0.887
Design value of C_L	1.390
Upper limit of C_L	1.885
Aerodynamic centre position	28.32% chord from leading edge 2.65% chord above chord line
Zero lift pitching moment coefficient	-0.128

These agree fairly well with the experimental values. For instance, in the case of the basic aerofoil at the largest Reynolds number, the following experimental results were obtained:

α_0	-6.4 degrees
$dC_L/d\alpha$	0.114
C_L at minimum profile drag	0.86

(although/

(although the lift coefficient can be reduced to 0.3 without serious drag penalty; i.e., the corresponding profile drag coefficient is around 0.015)

Upper limit of C_L 1.84
 Aerodynamic centre position 27.9% chord from leading edge
 0.7% chord above chord line

At the design lift coefficient, the pitching moment coefficient about the aerodynamic centre was -0.125.

4.1.2 Aerofoil with trip

There is again reasonable concurrence of experimental results with inviscid theory. For instance, at $R = 0.63 \times 10^6$, $dC_L/d\alpha$ was 0.114; C_L at minimum profile drag was 0.86; the upper limit of C_L was 1.88, which is nearer the theoretical value than that for the basic aerofoil; the aerodynamic centre was at 27.0% c, 0.3% c; the zero lift pitching moment coefficient might be around -0.150. The pitching moment coefficient about the aerodynamic centre at $C_L = 1.4$ was -0.115.

The minimum profile drag coefficients were somewhat lower at the smaller Reynolds numbers than those for the basic aerofoil. This can be seen from Table 6.

4.1.3 Aerofoil with flap

From thin aerofoil theory the increment in the lift coefficient obtained from flap deflection is

$$\Delta C_L = a_2 \delta \quad \dots(11)$$

where a_2 has in this case (i.e., for a ratio of flap chord to section chord of 0.1/1.1, namely 0.091) a value of 2.374. The calculated increments are given below together with the experimental values for the middle Reynolds number. The assumption that the lift coefficient without flap (although referred to the chord of aerofoil and flap) is the same as that with an extended flap at $\delta = 0$ may not be a good one since the trailing edge angle alters. There is, however, little indication that the slope of the lift curve increases with the addition of the flap.

Table 8

Flap angle δ degrees	-11.5	7.7	17.8	27.8
ΔC_L (theoretical) = 2.374 δ	-0.48	0.32	0.74	1.15
ΔC_L (experimental)	-0.36	0.20	0.42	0.54

As might be expected, the experimental values are smaller than the theoretical, with an increasing divergence as the magnitude of the flap deflection increases. The results, however, are quite remarkable in that the aerofoil is certainly not "thin" and has already a large camber without the addition of a flap. As can be seen from Fig.6, there is a fairly linear decrease in the stalling angle with increase in flap deflection. The decrement in stalling incidence is about 1 degree per 15 degrees of flap deflection. The maximum lift coefficient of 2.30 was obtained at the lowest Reynolds number with a flap angle of 27.8 degrees.

The theoretical value for the increment in pitching moment coefficient about the quarter chord can be estimated, again using thin aerofoil theory, from

$$\Delta C_{M_{c/4}} = - m\delta \quad \dots(12)$$

where m has a value of 0.209 for this particular case. The theoretical values are given below together with the experimental results; these have to be referred to the chord of the aerofoil with the flap. The assumption that an undeflected flap carries zero load may cause an error in the experimental values given below of as much as 10%.

Table 9

Flap angle δ degrees	-11.5	7.7	17.8	27.8
$\Delta C_{M_{c/4}}$ (theoretical) = $m\delta$	+0.042	-0.028	-0.065	-0.101
$\Delta C_{M_{c/4}}$ (experimental)	+0.063	-0.072	-0.107	-0.138

It can be seen that the experimental values are somewhat greater than the theoretical.

The addition of a flap did not increase the profile drag unduly. In fact there was in some cases a marked decrease in drag (Fig.7). This was particularly so at the lowest test speed. It would appear that a flap deflection of 15 to 20 degrees gives the highest ratios of lift to drag (Fig.14) at a Reynolds number around 0.5 million for this particular flap configuration.

4.2 Reynolds number effects

As can be seen from Fig.13, the small breadth wake associated with low profile drag could only be maintained above a certain limiting Reynolds number at each incidence. For instance, at an incidence of 6 degrees, the low drag characteristics could not be maintained below a Reynolds number of 0.35 million (if the wind speed was increasing), or 0.30 million (for decreasing wind speed). On the other hand, at an incidence of -4 degrees, the minimum Reynolds numbers had dropped to 0.20 million and 0.15 million respectively.

For the basic aerofoil, there was a general decrease in the profile drag coefficient with increase in Reynolds number which is in keeping with results from tests done on other aerofoils^{6,8}. For the aerofoil with flap, there appears to be a Reynolds number around 0.60×10^6 at which the profile drag coefficient is a minimum for the range of Reynolds number dealt with. For the majority of the configurations tested, the maximum lift coefficient tended to decrease slightly with increase in Reynolds number, Tables 4 and 5, for the range considered. From 3.3 it would seem that the aerodynamic centre moved aft and slightly upward (towards the theoretical point) with increase in Reynolds number.

4.3 Effect of boundary layer trip

As can be seen in Fig.15, a laminar separation bubble of about 4 cm length was formed on the upper surface of the aerofoil. Various forms of boundary layer trips were tried as follows.

Plastic sheet with an adhesive backing ("CON-TACT") was used to produce wedges with 6.5 mm sides and 0.25 mm thick. These were positioned with their bases 3 mm aft of tapping 7, pointing forward and with a spanwise pitch of 9.5 mm. This configuration was not as effective as that with 0.38 mm thick wedges having a similar base position and dimension, and pitch, but with a chordwise length of 30 mm. Strips of the same material with a breadth of 1.6 mm and 0.25 mm thickness were then arranged on the upper surface near tapping 7 in a variety of fashions. The length of each piece was 6.5 mm, and when arranged in a straight line, the gap between each pair was varied from 6.5 mm to 1 mm. None of these were as successful as a thread 0.13 mm diameter, allowing for the varnish used as an adhesive, or alternatively a strip of Con-tact 0.25 mm thick, 0.38 mm broad. These trips were positioned at about 3 mm forward of pressure tapping 7, i.e., at about 0.455 c from the aerofoil leading edge, measured along the chord; this appeared to be the optimum position.

The difference in size between the two most effective trips may be explained by the "hairy" nature of the thread as well as the difference in shape. The presence of the bubble caused the pressure in that region to increase linearly in the stream direction, Fig.9, but with the trip, Fig.10, this effect disappeared and the suction peak was moved further aft to the half-chord position. The trip seemed to have little effect on the lift characteristics of the aerofoil except at the high Reynolds number when slightly smaller values of lift coefficient were obtained with the trip than without it. At the two higher Reynolds numbers the trip gave a profile drag coefficient which was less than that for the basic aerofoil up to a lift coefficient of about 1.6, Fig.7. The trip did not appreciably alter the maximum lift, the stalling angle or the stall characteristics. At the highest Reynolds number, there seems some evidence, Fig.8, to suggest that the trip delayed the change in slope of the pitching moment curve until a lift coefficient of about 1.8 was reached.

4.4 Pressure distributions

The presence of the trip on the upper surface of the aerofoil appears to reduce the pressure, particularly on the lower surface and at lower incidences, Fig.9 and 10. This may be due to an increase in the effective thickness and camber of the aerofoil caused by the presence of the trip.

It is interesting to compare the theoretical pressure distributions with the experimental, Fig.11, at the design lift coefficient. The experimental values are almost always lower than the theoretical.

4.5 The stall

There was a certain value of incidence when the flow started to separate from the upper surface of the aerofoil near the trailing edge. With increase in incidence, the separation point moved forward until it reached some point near the mid-chord. Thus there was a rapid increase in drag which coincided with or just preceded, Tables 4 and 5, a more gradual decrease in lift. This was because there was still a fair suction over the forward part of the upper surface even after flow separation had taken place. The value of $d C_M / d C_L$ became infinite at the stall, Fig.8, and in the case of the aerofoil without flap the slope became strongly positive even before the stall. This implies a forward movement of the aerodynamic centre as the stall is approached.

4.6 Comparison of characteristics

Fig.14 shows that GU 25-5(11)8 compares favourably with NACA 63₄ - 420 fitted with 0.25 c slotted flap at 20 degrees as far as the lift and profile drag characteristics are concerned. It is possible that the profile drag coefficient of the NACA section would increase with reduction of Reynolds number to 0.5 million. The Wortmann section (FX 05-H-126) has a lower profile drag coefficient but the maximum lift coefficient is only about 1.2 compared with values around 2 obtained with the GU aerofoil. Also the maximum thickness to chord ratio of the Wortmann section is about 13% compared with 20% for the GU aerofoil. Fig.14 also shows the good correlation which exists between the results obtained for the GU aerofoil using the "Powell" program and experiment.

5. Acknowledgements

The test program could not have been accomplished without the assistance of the workshop technicians, Messrs. R. Carroll, C. Mathieson and R. Collins. Thanks are also due to some of our final year students who obtained the test data for the aerofoil with flap. The work done by T. Thorsteinsson during his final year project was particularly useful.

References/

References

<u>No.</u>	<u>Author(s)</u>	<u>Title, etc.</u>
1	T. Nonweiler	A new series of low drag aerofoils. University of Glasgow, Department of Aeronautics and Fluid Mechanics. Report No. 6801.
2	W. J. Duncan A. S. Thom and A. D. Young	Elementary treatise on the mechanics of fluids. Edward Arnold Ltd., 1960.
3	R. L. Maltby and R. F. A. Keating	Flow visualisation in low-speed wind tunnels. R.A.E. Tech. Note Aero. 2715. August, 1960.
4	-	British Standard 185: Part 1: 1950.
5	A. Pope and J. J. Harper	Low speed wind tunnel testing. John Wiley and Sons, Inc. 1966.
6	F. X. Wortmann	Experimentelle Untersuchungen an neuen Laminarprofilen für Segelflugzeuge und Hubschrauber. Z. Flugwiss 5. Heft 8, 228, 1957.
7	J. J. Spillman	Design philosophy of man-powered aircraft. J. R. Ae. S., Vol. 66, November, 1962.
8	I. H. Abbott and A. E. von Doenhoff	Theory of wing sections. McGraw Hill Book Company, Inc. 1949.
9	B. J. Powell	The calculation of the pressure distribution on a thick cambered aerofoil at subsonic speeds including the effect of the boundary layer. NPL Aero Report 1238, June, 1967 ARC C.P.No.1005.

Appendix 1

GU 25-5(11)8.

Complete set of Co-ordinate Data

X	Y	KI (DEG)	THETA (DEG)	q_α		q_α AT INCIDENCE OF LOW-DRAG RANGE		
				$\cos(\theta/2-\alpha)$	LOWER LIMIT	DESIGN	UPPER LIMIT	
1.000 00	0.000 00	-18.64	0.00	0.000	0.000	0.000	0.000	
0.950 00	0.018 15	-20.22	22.39	0.914	0.911	0.914	0.912	
0.900 00	0.036 02	-19.58	32.90	0.988	0.974	0.983	0.987	
0.850 00	0.054 13	-20.24	41.33	1.057	1.027	1.042	1.052	
0.800 00	0.072 82	-20.68	48.88	1.140	1.088	1.109	1.125	
0.750 00	0.091 73	-20.67	55.99	1.238	1.156	1.184	1.206	
0.700 00	0.110 37	-20.12	62.87	1.354	1.233	1.269	1.299	
0.650 00	0.128 15	-18.90	69.69	1.492	1.320	1.365	1.404	
0.600 00	0.144 34	-16.81	76.55	1.658	1.417	1.474	1.523	
0.550 00	0.158 00	-13.46	83.54	1.859	1.527	1.597	1.660	
0.500 00	0.167 50	-6.94	90.76	2.085	1.634	1.721	1.799	
0.450 00	0.170 84	-1.22	97.94	2.169	1.612	1.710	1.799	
0.400 00	0.170 03	2.95	105.02	2.267	1.589	1.698	1.799	
0.350 00	0.165 82	6.63	112.12	2.385	1.563	1.685	1.799	
0.300 00	0.158 44	10.16	119.36	2.529	1.534	1.670	1.799	
0.250 00	0.147 87	13.73	126.88	2.711	1.499	1.653	1.799	
0.200 00	0.133 88	17.58	134.85	2.949	1.456	1.631	1.799	
0.150 00	0.115 93	22.02	143.56	3.283	1.399	1.603	1.799	
0.100 00	0.092 91	27.68	153.52	3.801	1.315	1.561	1.799	
0.075 00	0.078 76	31.45	159.30	4.201	1.253	1.529	1.799	
0.050 00	0.061 99	36.51	166.05	4.807	1.161	1.483	1.799	
0.025 00	0.040 82	44.69	174.69	5.930	0.995	1.400	1.799	
0.005 00	0.015 52	61.41	185.92	8.622	0.607	1.206	1.799	
0.000 00	0.000 00	90.00	194.46	13.267	-0.053	0.873	1.794	
0.005 00	-0.009 64	141.20	202.02	11.506	-0.805	-0.002	0.801	
0.025 00	-0.018 19	166.30	211.42	6.449	-0.977	-0.530	-0.080	
0.050 00	-0.022 62	172.45	218.49	4.604	-0.977	-0.660	-0.341	
0.075 00	-0.025 32	174.94	224.00	3.773	-0.977	-0.720	-0.460	
0.100 00	-0.027 20	176.38	228.73	3.273	-0.977	-0.756	-0.532	
0.150 00	-0.029 56	178.04	236.86	2.673	-0.977	-0.801	-0.621	
0.200 00	-0.030 80	179.03	243.95	2.313	-0.977	-0.828	-0.675	
0.250 00	-0.031 33	179.73	250.43	2.066	-0.977	-0.847	-0.714	
0.300 00	-0.031 31	180.30	256.50	1.883	-0.977	-0.862	-0.743	
0.350 00	-0.030 81	180.83	262.31	1.740	-0.977	-0.874	-0.767	
0.400 00	-0.029 85	181.41	267.95	1.624	-0.977	-0.884	-0.787	
0.450 00	-0.028 26	182.18	273.48	1.518	-0.971	-0.887	-0.799	
0.500 00	-0.026 16	182.58	278.92	1.424	-0.961	-0.885	-0.806	
0.550 00	-0.023 81	182.80	284.33	1.342	-0.952	-0.884	-0.811	
0.600 00	-0.021 31	182.91	289.77	1.271	-0.943	-0.881	-0.815	
0.650 00	-0.018 75	182.93	295.29	1.208	-0.934	-0.879	-0.819	
0.700 00	-0.016 21	182.88	300.97	1.152	-0.926	-0.876	-0.822	
0.750 00	-0.013 74	182.77	306.89	1.101	-0.918	-0.873	-0.824	
0.800 00	-0.011 37	182.63	313.21	1.055	-0.910	-0.870	-0.827	
0.850 00	-0.009 13	182.51	320.13	1.012	-0.902	-0.868	-0.830	
0.900 00	-0.006 94	182.59	328.09	0.971	-0.895	-0.866	-0.833	
0.950 00	-0.004 10	184.27	338.20	0.911	-0.867	-0.846	-0.820	
1.000 00	-0.000 00	184.57	360.00	0.000	0.000	0.000	0.000	

Appendix 2

Data Corrections

Incidence

By using a symmetrical aerofoil, it was found that the flow in the tunnel working section was yawed by 0.6 degree in the same plane as the test incidence was measured. Hence the corrected incidence was obtained by adding 0.6 degree to the geometric incidence. i.e.

$$\alpha' = \alpha_{geom.} + 0.6 \quad \dots(A.1)$$

It was also found that the normal pressure drag coefficients were usually much larger than the boundary layer drag coefficients obtained from the wake survey. This was especially so for the higher lift coefficients. The total normal pressure drag consists of the sum of the form drag (which is the profile drag less the surface friction) and the vortex drag⁴. The general magnitude of the surface friction is found by using the rough rule²,

$$\text{form drag: profile drag} = t:c \quad \dots(A.2)$$

Thus for a profile drag coefficient of 0.015 (which is a fairly representative value for the aerofoil under test), the form drag coefficient will have a value of approximately 0.003 and the surface friction drag coefficient will be 0.012. Since the values obtained for the pressure drag coefficient under these circumstances ($C_L = 1.6$) were around 0.050, it would appear that there was considerable vortex drag. This was substantiated by using oil film techniques and also by measuring the total lift and drag by means of a balance. It could then be stated that

$$C_{D_v} = C_{D_p} - C'_D + 0.01, \quad \dots(A.3)$$

where the surface friction drag coefficient has been given a constant value. An incidence correction could then be arrived at using

$$\alpha_e = \alpha' - C'_D / C'_L \quad \dots(A.4)$$

The correction in incidence obtained by these means was of the order of one degree.

The final correction applied to the incidence was that associated with streamline curvature and was obtained from Ref.5. For the particular wind tunnel used, the expression was

$$\alpha^0 = \alpha_e^0 + 0.133 (C'_L + 4 C'_{M_{c/4}}) \quad \dots(A.5)$$

and the actual correction was of the order of 0.1 degree. When one considers that the error in incidence setting might have been ± 0.2 degree, the above correction is practically negligible.

Lift and pitching moment

The corrections applied were associated with streamline curvature, solid and wake blockage and for the particular set-up the expressions were:

$$C_L = 0.972 C'_L \quad \dots(A.6)$$

$$C_{M_{c/4}} = 0.987 C'_{M_{c/4}} \quad \dots(A.7)$$

These corrections are again small when compared with experimental error.

Drag

In order to arrive at a correction of the pressure drag due to the buoyancy effect, the longitudinal static pressure gradient in the working section was ascertained experimentally. This was done by using a static pressure probe located along the centre-line. For this particular model the incremental buoyancy drag coefficient had a value of around 0.0005, varying with the speed setting.

The expression for the corrected profile drag coefficient was

$$C_D = 0.981 C'_D \quad \dots(A.8)$$

when solid and wake blockage corrections are incorporated.



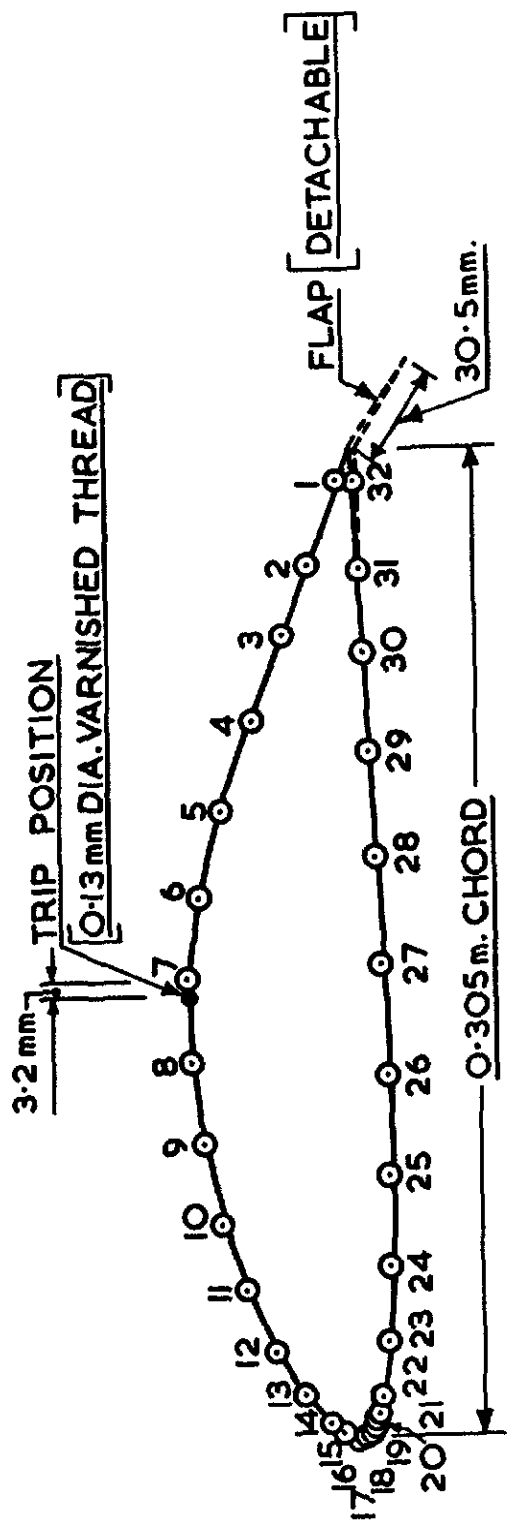


Fig. 1. 0.305 m. CHORD AEROFOIL SHOWING PRESSURE TAPPING POSITIONS.

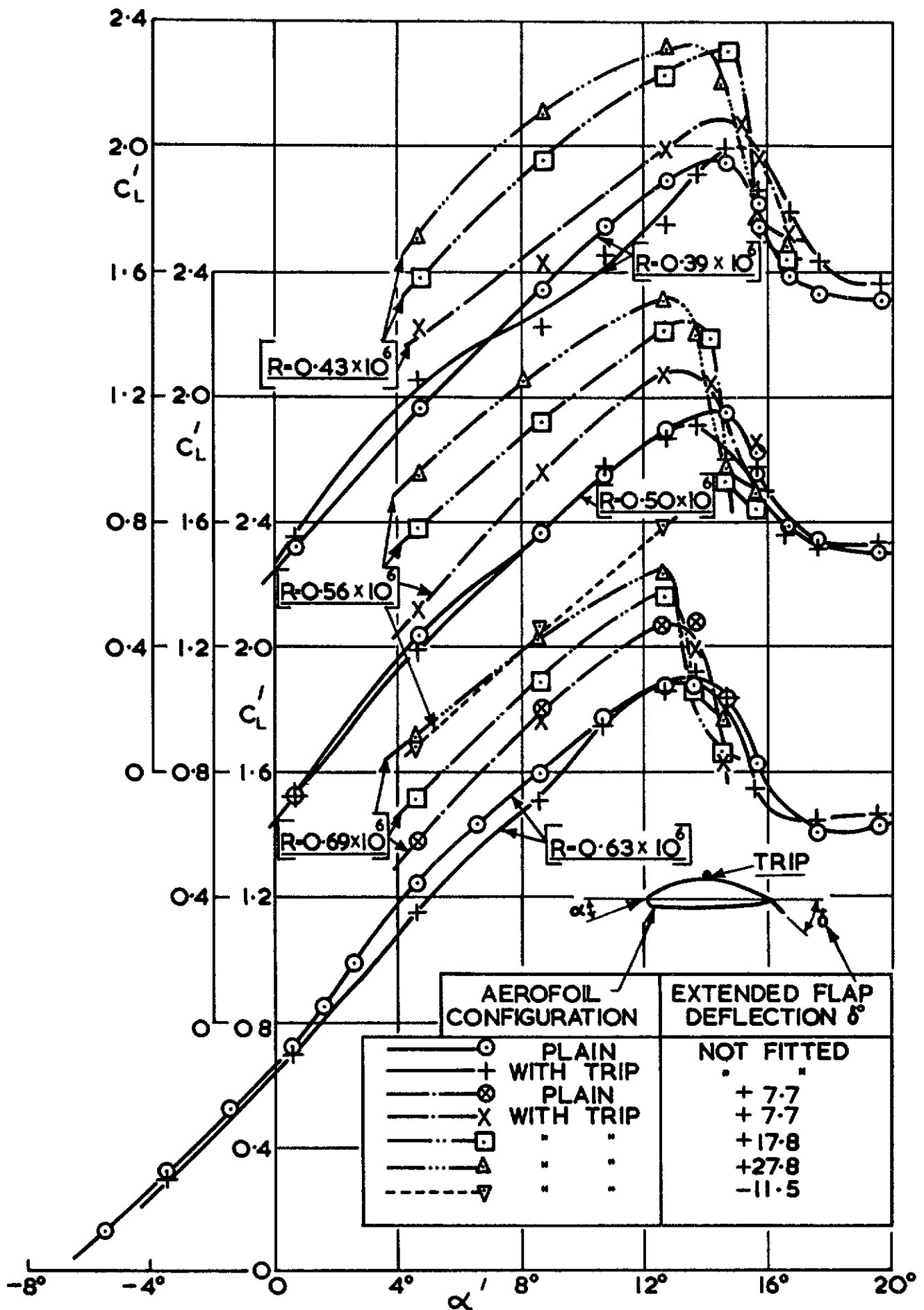


Fig. 2. LIFT COEFFICIENT v.s. α'

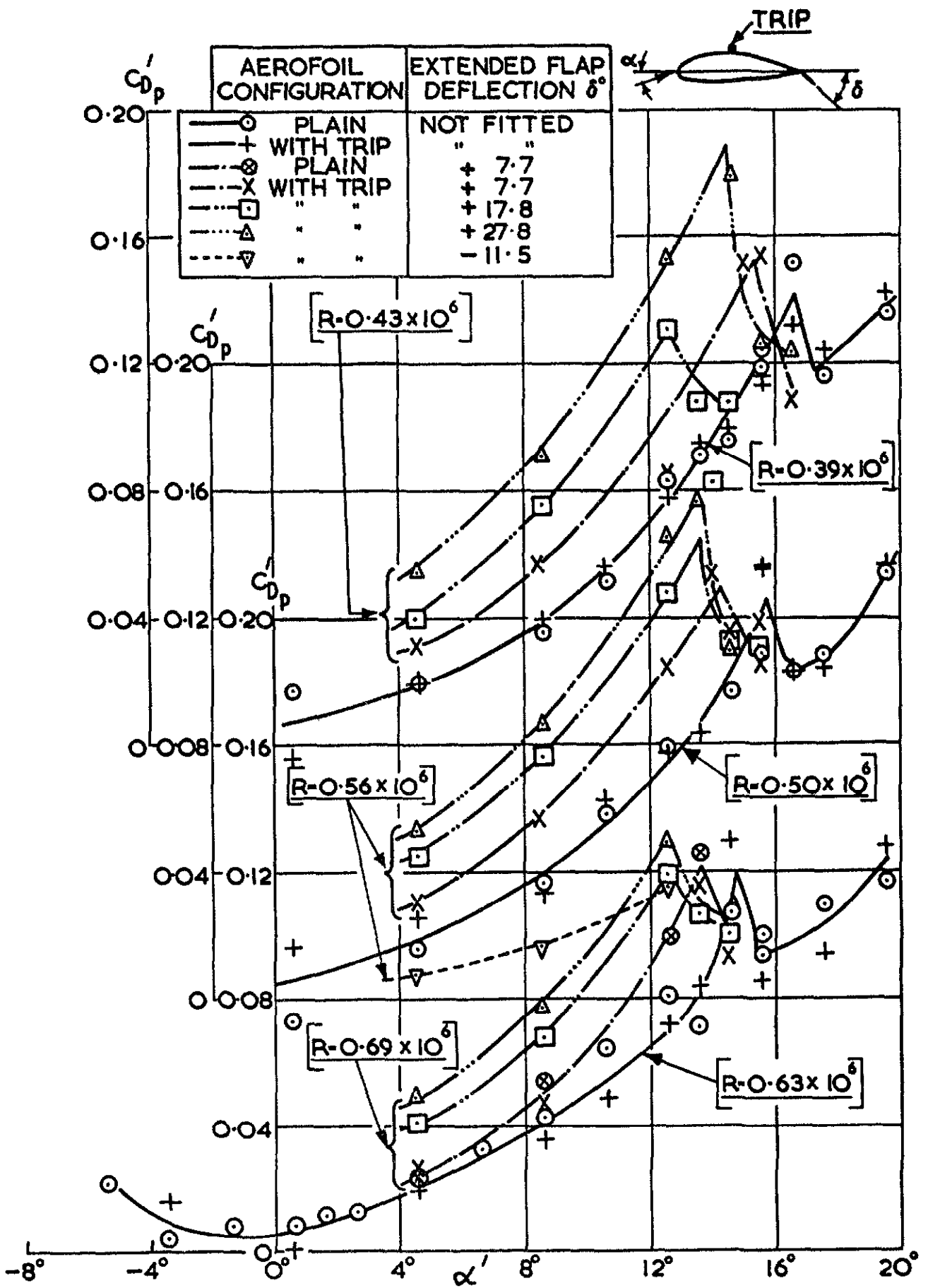


Fig. 3. PRESSURE DRAG COEFF. vs α'

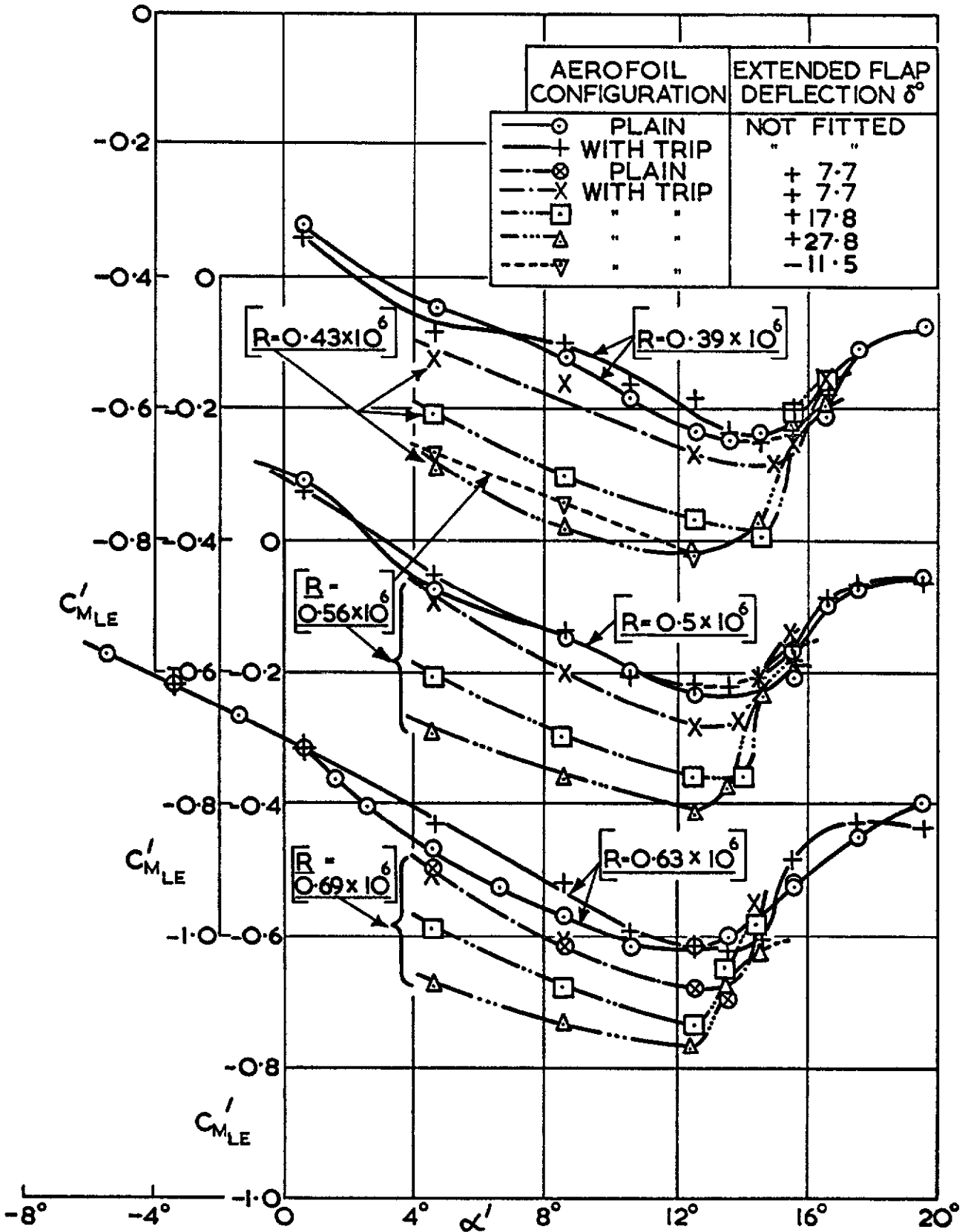
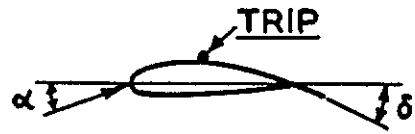


Fig.4. MOMENT COEFFICIENT ABOUT LEADING EDGE vs α'

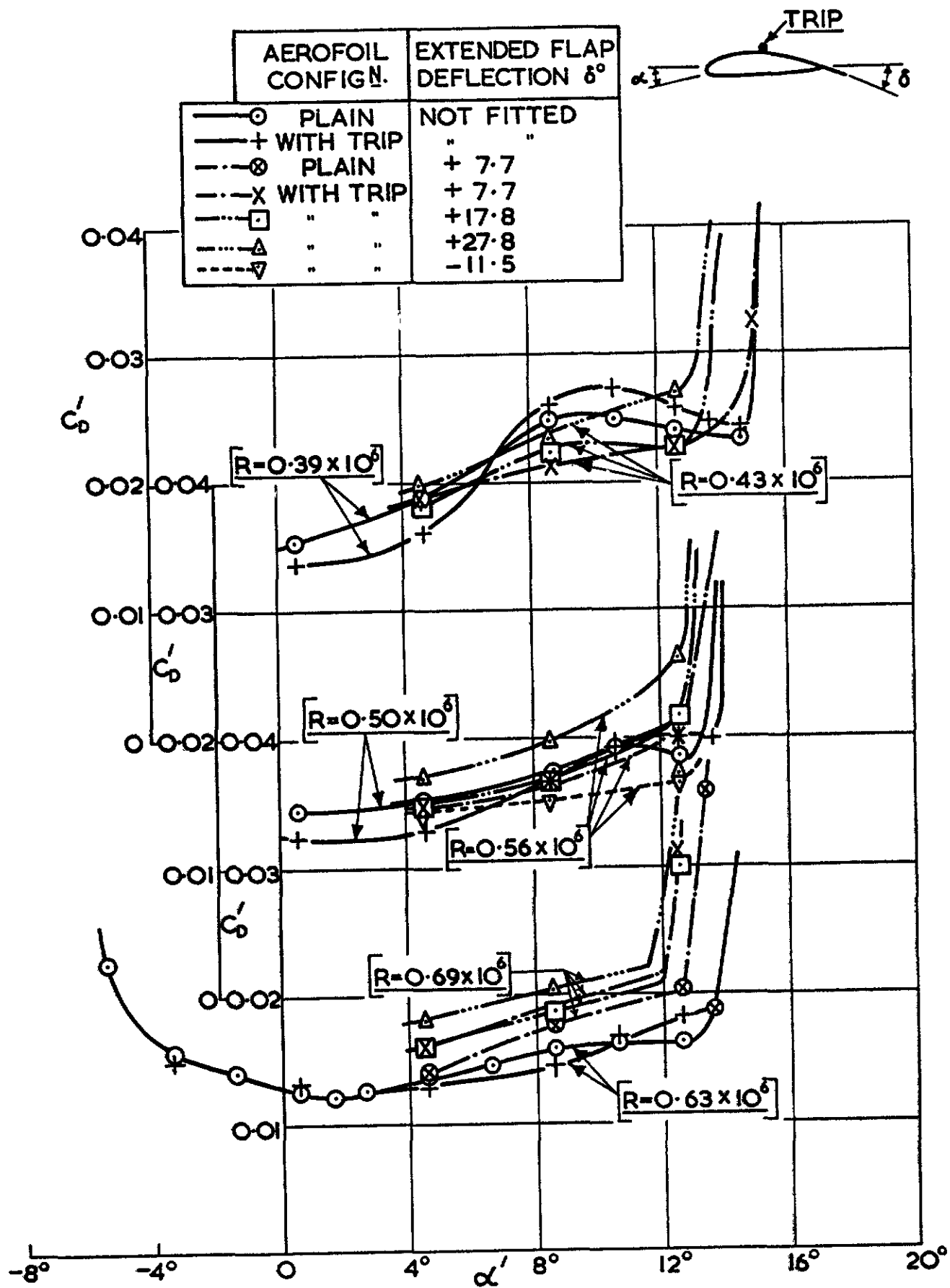


Fig. 5. PROFILE DRAG COEFF. vs α'

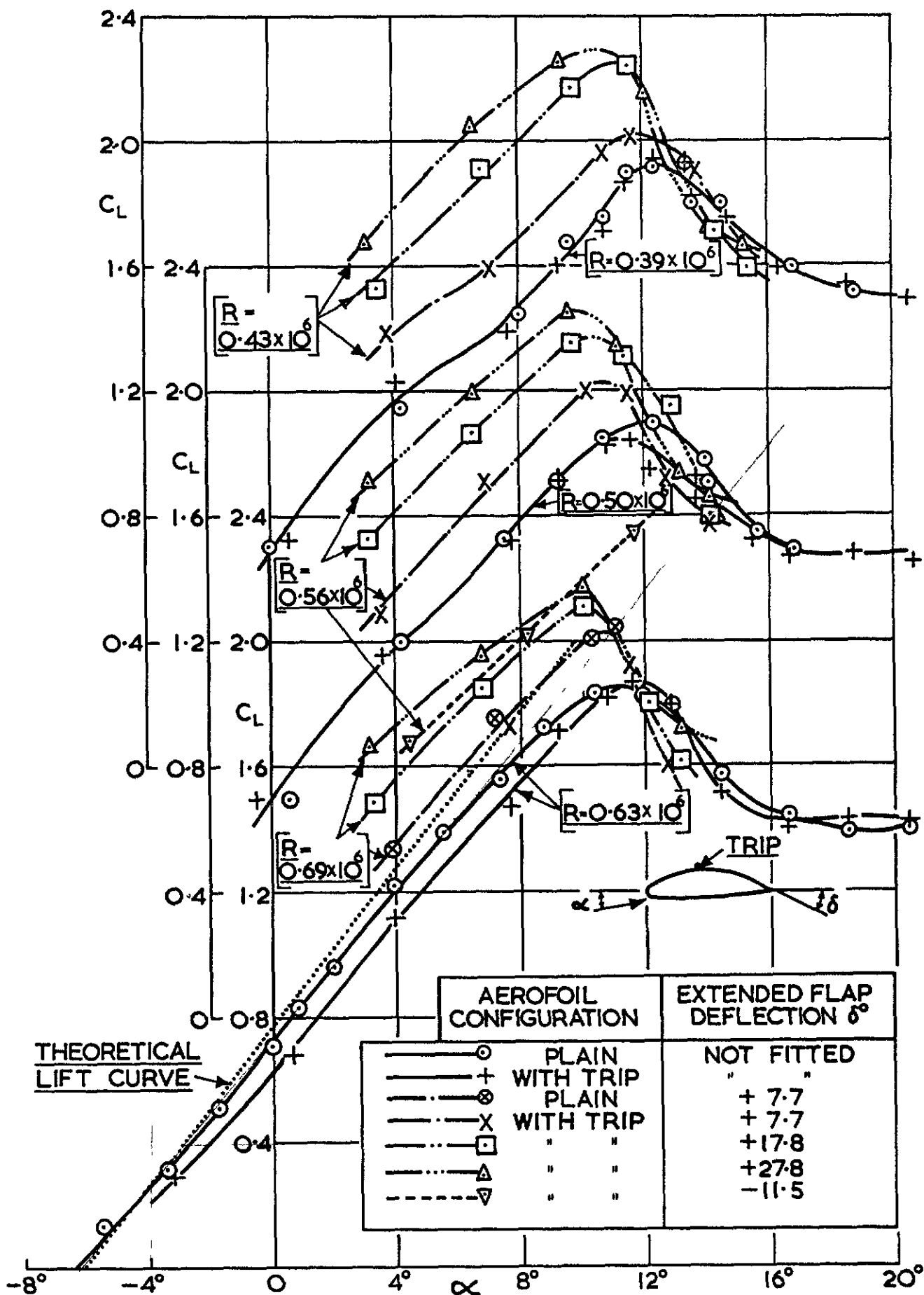


Fig. 6. LIFT COEFFICIENT (CORRECTED) v.s. α

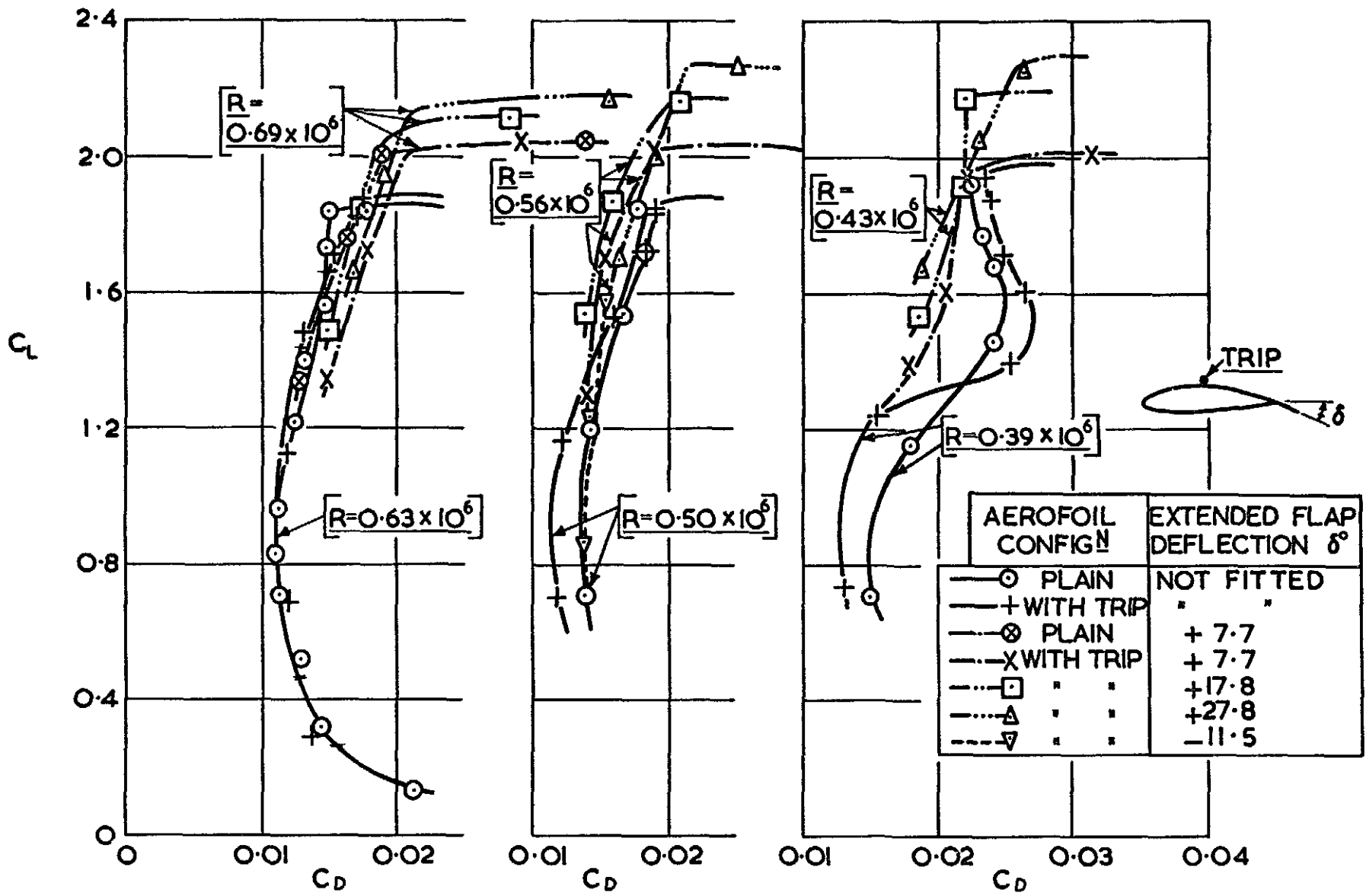
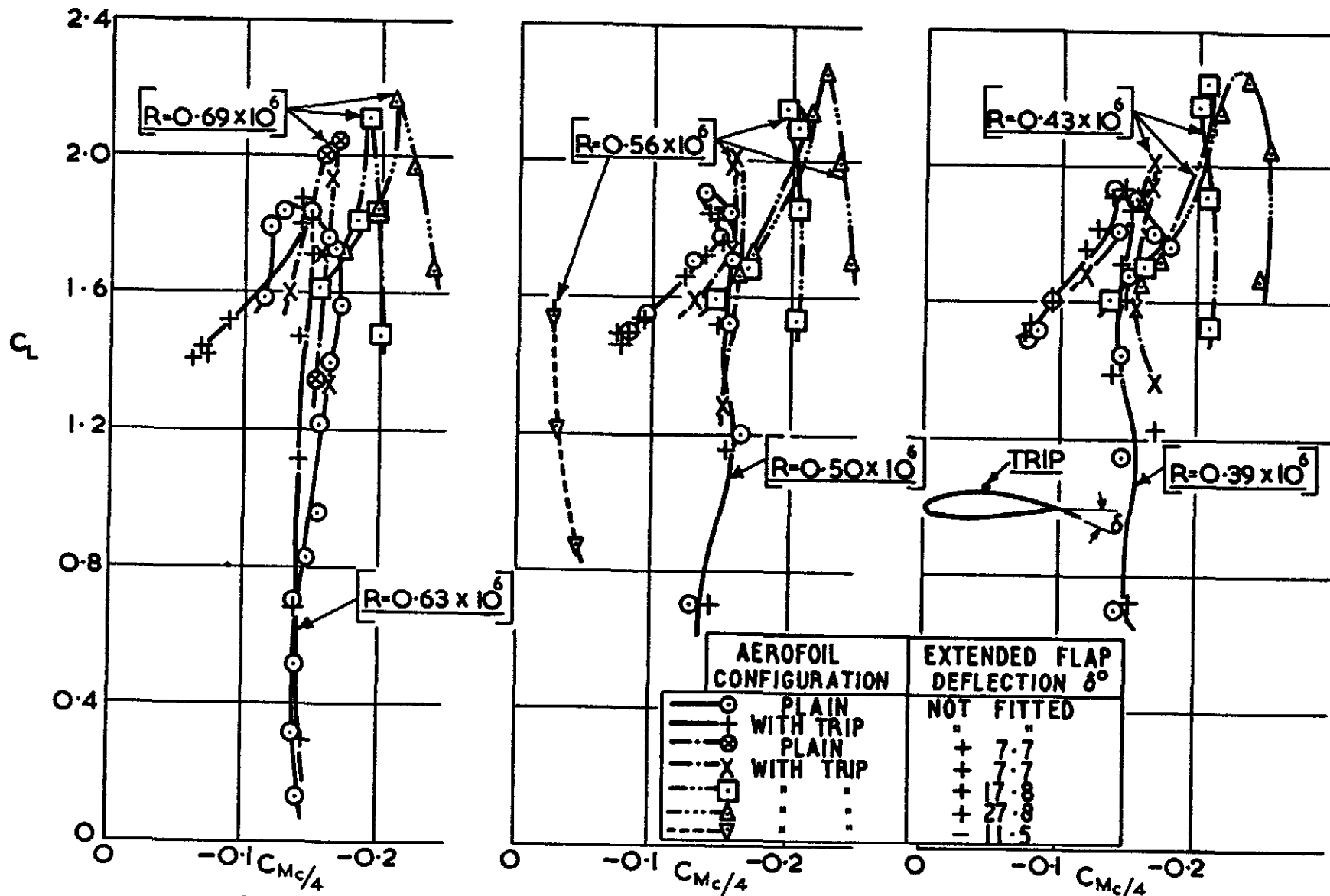


Fig. 7. PROFILE DRAG COEFF. [CORRECTED] vs LIFT COEFF. [CORRECTED]



**Fig.8. MOMENT COEFF. ABOUT QUARTER CHORD (CORRECTED)
vs. LIFT COEFF. (CORRECTED.)**

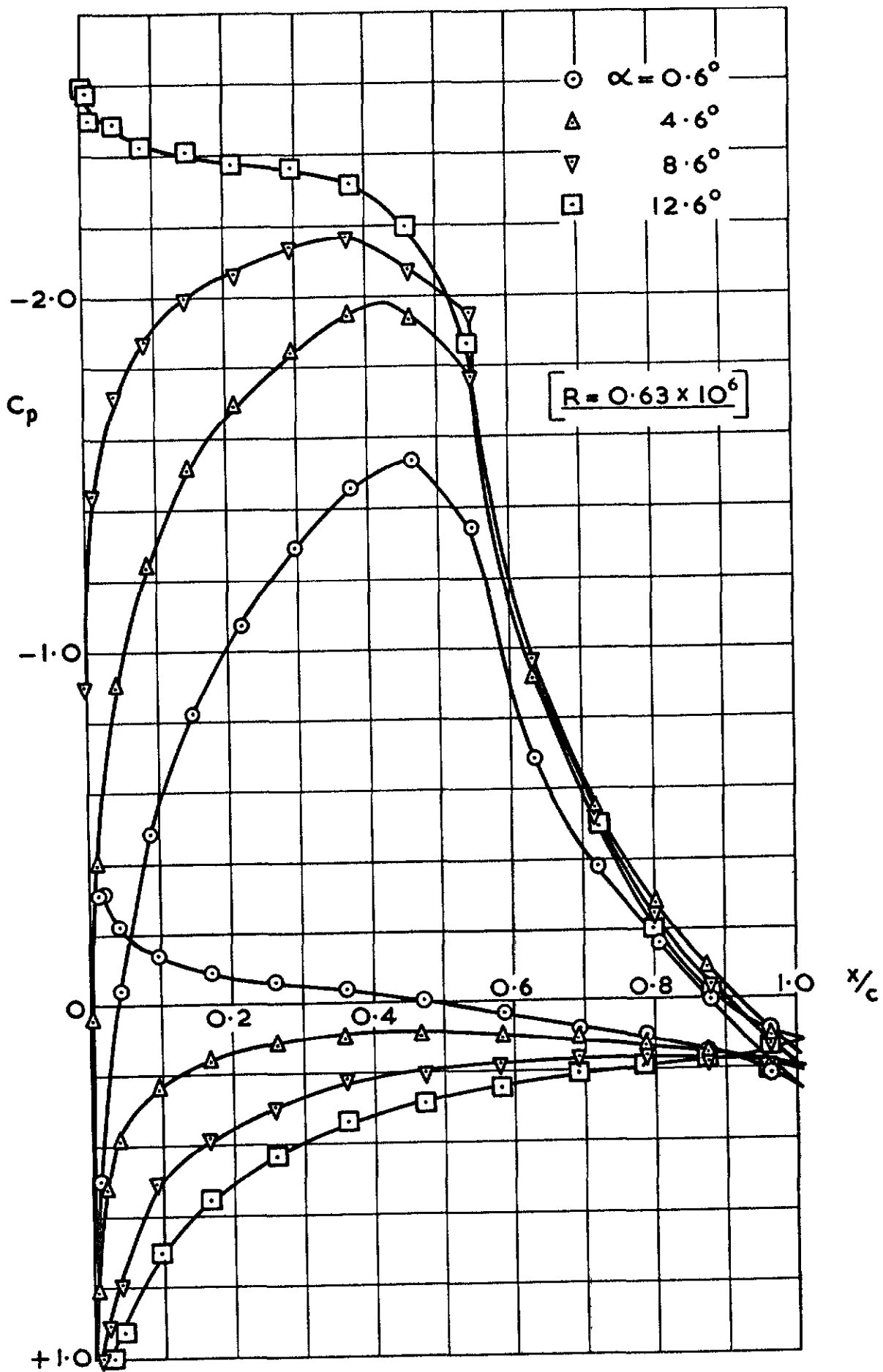


Fig. 9. EXPERIMENTAL PRESSURE DISTRIBUTIONS
— PLAIN AEROFOIL.

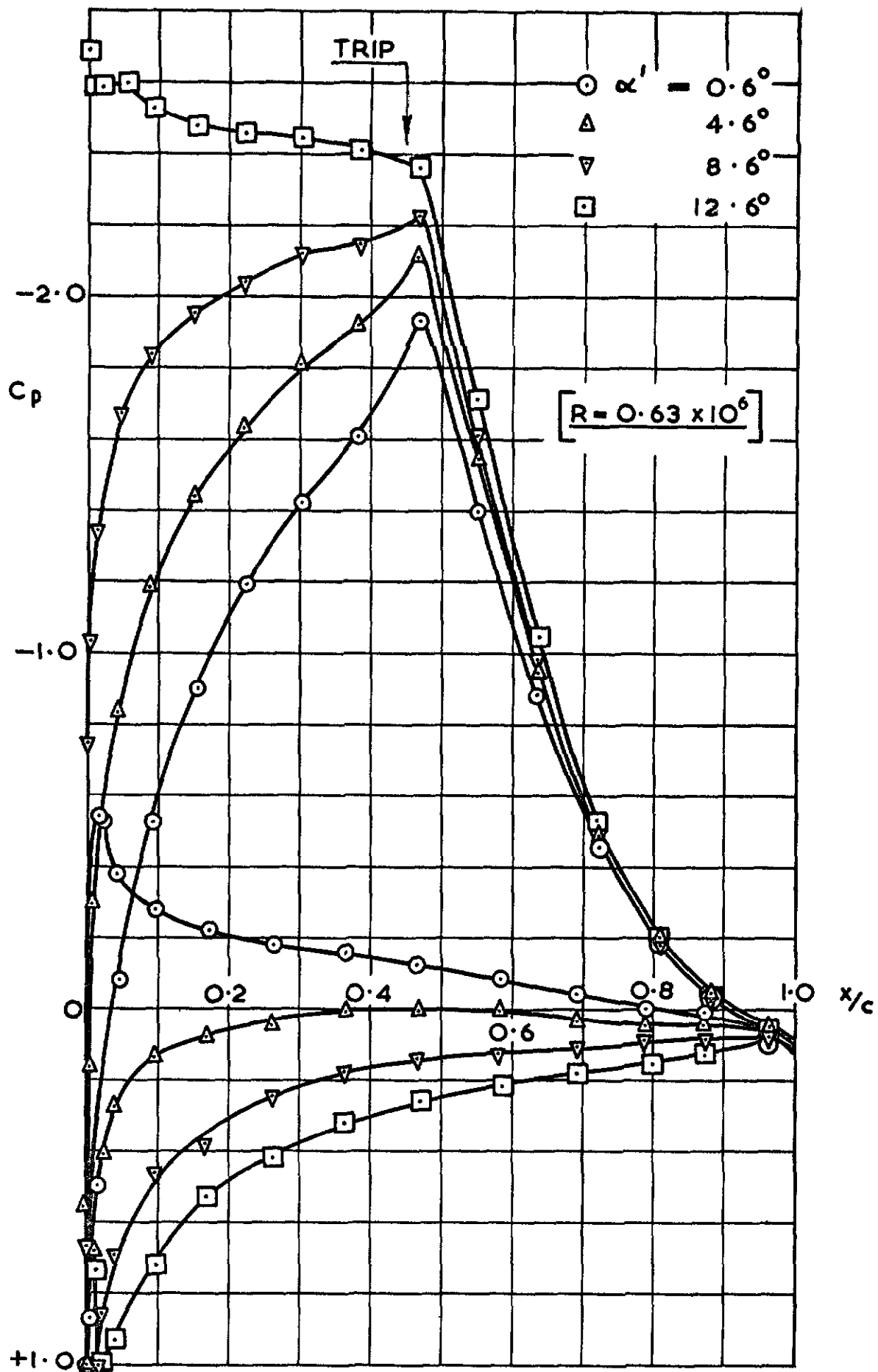
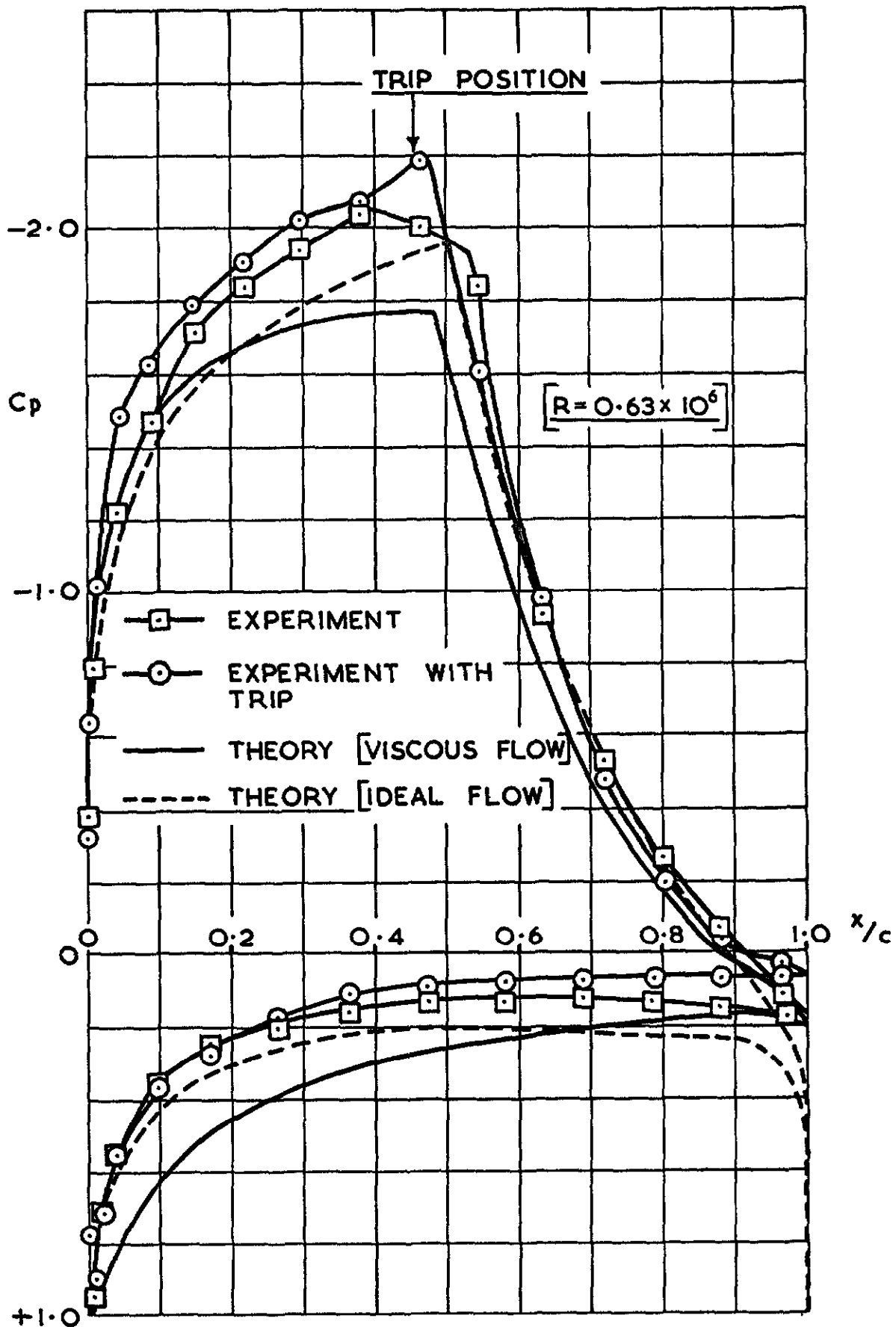


Fig.10. EXPERIMENTAL PRESSURE DISTRIBUTIONS AEROFOIL WITH UPPER SURFACE TRIP.



**Fig.II. EXPERIMENT AND THEORY COMPARISON
PRESSURE PLOT FOR DESIGN $C_L = 1.39$**

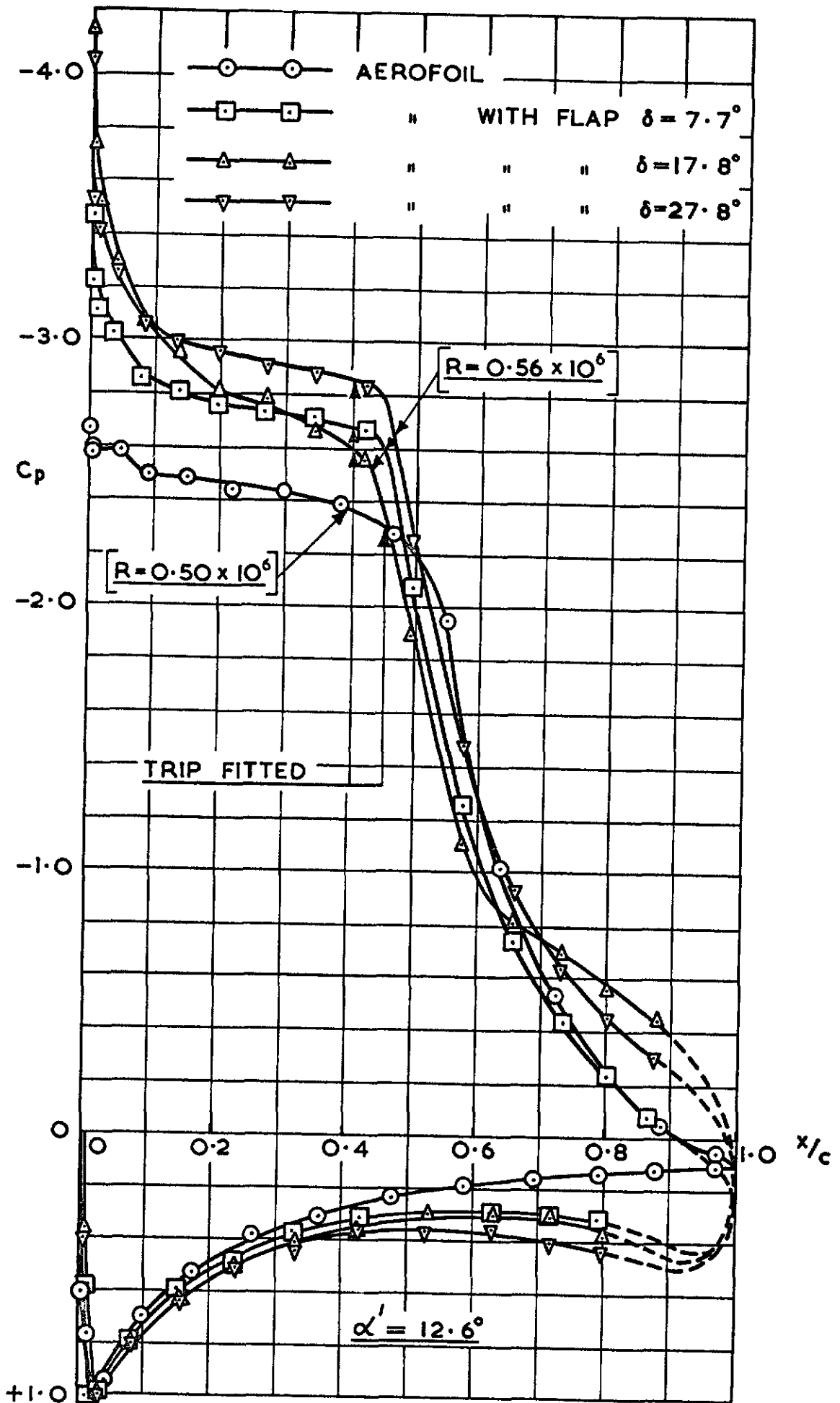


Fig.12. EXPERIMENTAL PRESSURE DISTRIBUTIONS AEROFOIL WITH VARIOUS FLAP SETTINGS.

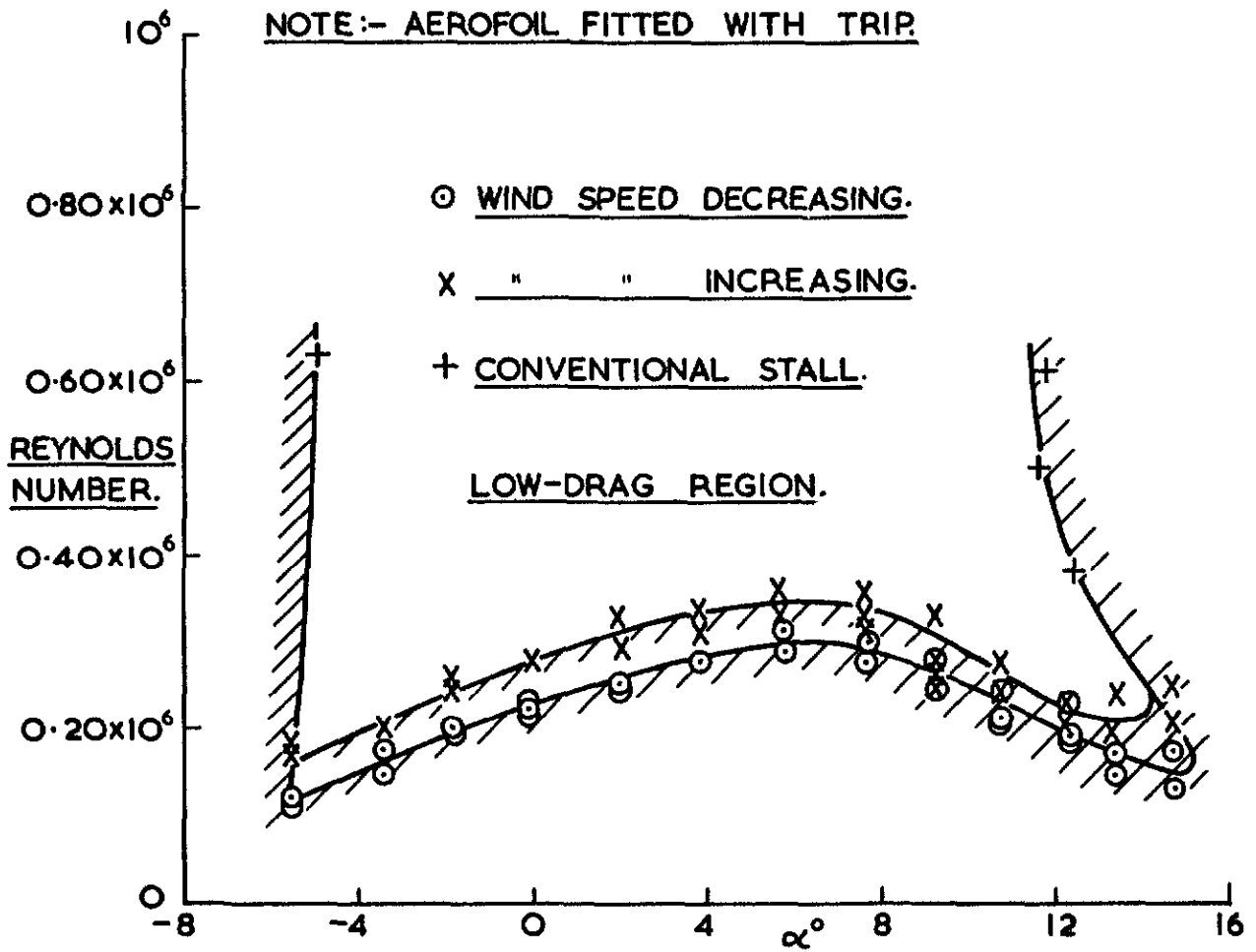


Fig. 13. REYNOLDS NUMBER WHEN WAKE CHARACTERISTICS CHANGE vs. α

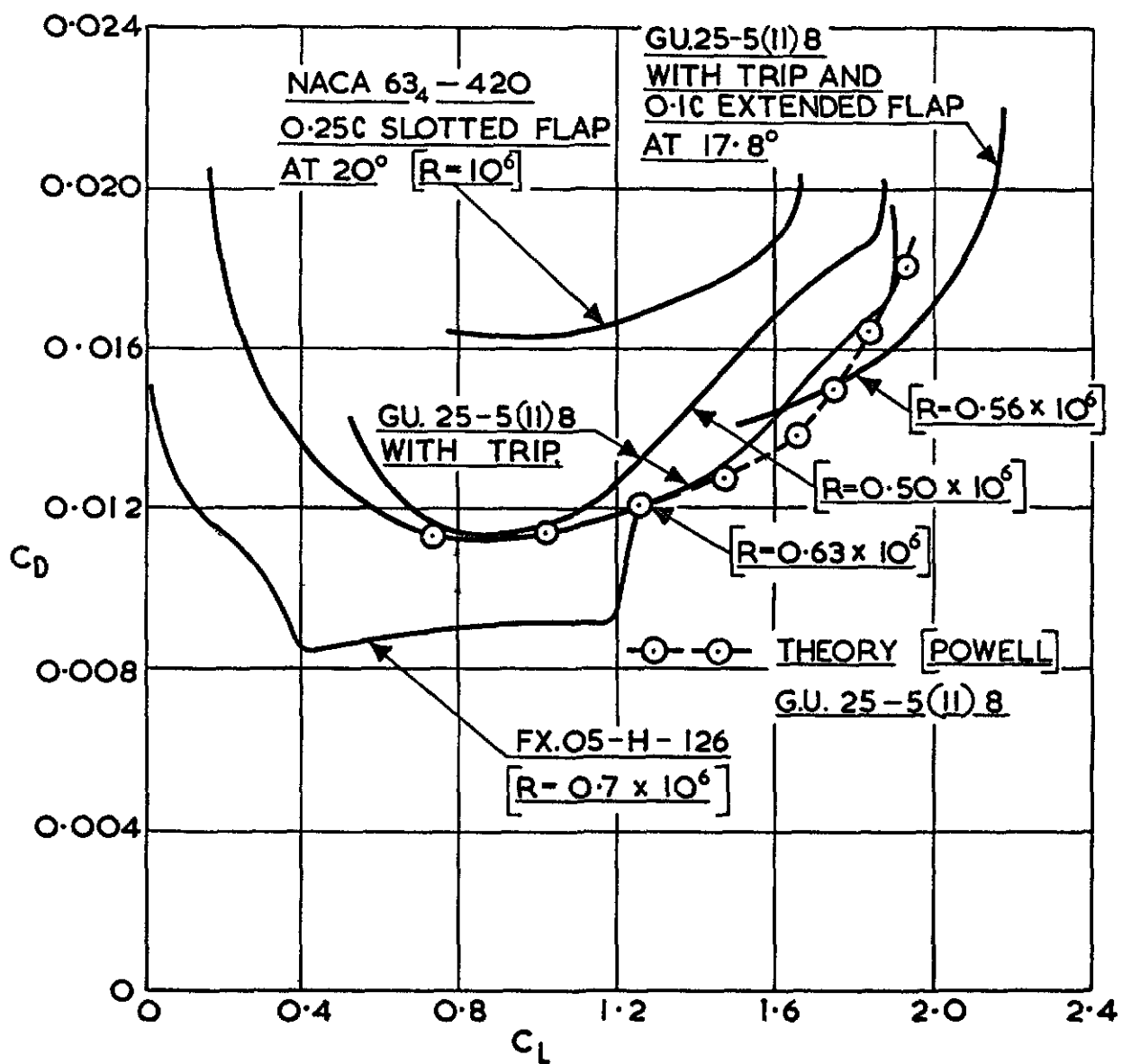


Fig.14. COMPARISON OF GU25-5(II)8 LIFT DRAG CHARACTERISTICS WITH THOSE OF OTHER AEROFOILS.

A.R.C. C.P.No.1187
September, 1968

F. H. Kelling

EXPERIMENTAL INVESTIGATION OF A HIGH-LIFT
LOW-DRAG AEROFOIL

One of a series of low-drag aerofoils¹ designated GU 25-5(11)8 was selected for low speed wind tunnel testing at Reynolds numbers around half a million. Coefficients of lift, drag and pitching moment were obtained for a range of incidence, using a two-dimensional wing. The maximum section lift coefficient obtained was 1.93 and the minimum profile drag coefficient was 0.0112. Results compared favourably with those deduced theoretically. The addition of a boundary layer trip to the upper surface caused the profile drag to decrease at/

A.R.C. C.P.No.1187
September, 1968

F. H. Kelling

EXPERIMENTAL INVESTIGATION OF A HIGH-LIFT
LOW-DRAG AEROFOIL

One of a series of low-drag aerofoils¹ designated GU 25-5(11)8 was selected for low speed wind tunnel testing at Reynolds numbers around half a million. Coefficients of lift, drag and pitching moment were obtained for a range of incidence, using a two-dimensional wing. The maximum section lift coefficient obtained was 1.93 and the minimum profile drag coefficient was 0.0112. Results compared favourably with those deduced theoretically. The addition of a boundary layer trip to the upper surface caused the profile drag to decrease at/

A.R.C. C.P.No.1187
September, 1968

F. H. Kelling

EXPERIMENTAL INVESTIGATION OF A HIGH-LIFT
LOW-DRAG AEROFOIL

One of a series of low-drag aerofoils¹ designated GU 25-5(11)8 was selected for low speed wind tunnel testing at Reynolds numbers around half a million. Coefficients of lift, drag and pitching moment were obtained for a range of incidence, using a two-dimensional wing. The maximum section lift coefficient obtained was 1.93 and the minimum profile drag coefficient was 0.0112. Results compared favourably with those deduced theoretically. The addition of a boundary layer trip to the upper surface caused the profile drag to decrease at/

at some incidences. At the design lift coefficient of 1.4, the ratio of lift to profile drag was 108 at a Reynolds number of 0.63 million. The addition of an extended, sealed, flat-plate flap, with a chord one tenth that of the aerofoil, at the trailing edge of the aerofoil gave favourable results. A maximum ratio of lift to profile drag of 116 was obtained at a lift coefficient of 1.8 with a flap deflection of 17.8 degrees, while the maximum lift coefficient achieved was 2.30.

at some incidences. At the design lift coefficient of 1.4, the ratio of lift to profile drag was 108 at a Reynolds number of 0.63 million. The addition of an extended, sealed, flat-plate flap, with a chord one tenth that of the aerofoil, at the trailing edge of the aerofoil gave favourable results. A maximum ratio of lift to profile drag of 116 was obtained at a lift coefficient of 1.8 with a flap deflection of 17.8 degrees, while the maximum lift coefficient achieved was 2.30.

at some incidences. At the design lift coefficient of 1.4, the ratio of lift to profile drag was 108 at a Reynolds number of 0.63 million. The addition of an extended, sealed, flat-plate flap, with a chord one tenth that of the aerofoil, at the trailing edge of the aerofoil gave favourable results. A maximum ratio of lift to profile drag of 116 was obtained at a lift coefficient of 1.8 with a flap deflection of 17.8 degrees, while the maximum lift coefficient achieved was 2.30.



Fig. 15 Photograph of Aerofoil Upper Surface with Oil Film, 10° Incidence, 0.63×10^6 R.N.

© *Crown copyright* 1971

Produced and published by
HER MAJESTY'S STATIONERY OFFICE

To be purchased from
49 High Holborn, London WC1V 6HB
13a Castle Street, Edinburgh EH2 3AR
109 St Mary Street, Cardiff CF1 1JW
Brazennose Street, Manchester M60 8AS
50 Fairfax Street, Bristol BS1 3DE
258 Broad Street, Birmingham B1 2HE
80 Chichester Street, Belfast BT1 4JY
or through booksellers

Printed in England